Journal of Quality Measurement and Analysis *JQMA* 22(SI) 2026, 105-128
e-ISSN: 2600-8602 *http://www.ukm.my/jqma*
https://doi.org/10.17576/jqma.22si.2026.07

ANALYSIS OF ASYMMETRICAL ROCK-PAPER-SCISSORS (RPS) COMPETITION MODEL IN HETEROGENEOUS ENVIRONMENTS

(*Analisis Model Persaingan Asimetri Batu-Kertas-Gunting (RPS) dalam Persekitaran Heterogen*)

TASIU ABDULLAHI YUSUF & MOHD HAFIZ MOHD*

ABSTRACT

Asymmetrical rock-paper-scissors (RPS) competition refers to a dynamical system where species interact in a cyclic dominance pattern, but with unequal strengths or advantages. In the RPS models, three species interact such that each one outcompetes another, creating asymmetrical interactions that prevent any single species from dominating indefinitely. This competitive asymmetry phenomenon can arise due to the differences in reproduction rates, survival probabilities, or environmental factors that favour one species over another. Thus, understanding the factors driving community dynamics and coexistence mechanisms of multiple species is an important goal in ecology. In this paper, we examine the RPS competition framework extended along an environmental gradient. We formulate an extended system of nonlinear differential equations to capture asymmetrical RPS interactions under varying environmental conditions. Analytical techniques, including the evaluation of equilibrium points and linear stability analysis, are employed to determine stability and long-term dynamics of the system. In addition, numerical simulations are conducted to explore dynamical behaviours such as distinct steady states, limit cycles and heteroclinic cycles across environmental gradients. Our results reveal a variety of ecological outcomes driven by the interplay of asymmetrical RPS interactions and varying environmental conditions. Specifically, we demonstrate the emergence of distinct steady states, including scenarios where only a single-species persists, two-species coexistence, as well as the occurrence of multi-species coexistence. Additionally, stable limit cycles can occur, which indicate periodic fluctuations in species abundances. We also discover the presence of heteroclinic cycles, suggesting transient dynamics where species sequentially dominate before eventually returning to a similar state, and alternative stable states, where the final community composition depends on initial conditions. Ecologically, these findings highlight that the joint influences of RPS competitive asymmetries and environmental heterogeneity can lead to different community structures and ecological dynamics.

Keywords: asymmetrical competition; ecological modeling; heterogeneous environment; rock-paper-scissors (RPS) dynamics

ABSTRAK

Persaingan asimetri batu-kertas-gunting (RPS) merujuk kepada sistem dinamik yang mana spesies berinteraksi melalui corak dominasi kitaran, tetapi dengan kekuatan interaksi yang tidak seimbang. Dalam model RPS, tiga spesies berinteraksi sedemikian rupa sehingga setiap spesies mengatasi satu sama lain dan pada masa yang sama ditewaskan oleh spesies ketiga, sekali gus membentuk struktur interaksi asimetri yang menghalang penguasaan mutlak oleh mana-mana spesies. Persaingan asimetri ini boleh berpunca daripada perbezaan kadar pertumbuhan, kebarangkalian kemandirian, atau faktor persekitaran yang memberikan kelebihan relatif kepada spesies tertentu. Oleh itu, pemahaman terhadap mekanisme yang mengawal dinamik komuniti dan mekanisme hidup bersama pelbagai spesies merupakan isu penting dalam kajian ekologi. Dalam makalah ini, kami mengkaji rangka kerja persaingan asimetri RPS yang digabungkan dengan kecerunan persekitaran. Satu sistem persamaan pembezaan biasa tak linear dirumuskan bagi memodelkan interaksi asimetri RPS di bawah keadaan persekitaran yang berubah-ubah. Analisis matematik, termasuk penentuan titik keseimbangan dan analisis

kestabilan linear, digunakan untuk mengkaji kestabilan serta tingkah laku jangka panjang sistem. Di samping itu, simulasi berangka dijalankan bagi meneroka pelbagai dinamik, seperti keadaan mantap, kitaran had dan kitaran heteroklinik merentasi kecerunan persekitaran. Dapatan kajian menunjukkan kepelbagaian dinamik ekologi yang didorong oleh gabungan persaingan asimetri RPS dan persekitaran heterogen. Secara khusus, kami mengenal pasti kewujudan pelbagai keadaan mantap, termasuk kemandirian satu spesies, koeksistensi dua spesies, serta koeksistensi berbilang spesies. Selain itu, kitaran had stabil turut diperhatikan, yang mencerminkan turun naik berkala dalam saiz populasi suatu spesies. Kajian ini juga mendedahkan kehadiran kitaran heteroklinik, yang menggambarkan dinamik sementara yang mana spesies mendominasi secara bergilir-gilir sebelum sistem kembali menghampiri keadaan yang hampir serupa, serta kewujudan keadaan stabil alternatif yang bergantung kepada syarat awal. Dari perspektif ekologi, dapatan ini menekankan bahawa interaksi antara persaingan asimetri RPS dan persekitaran heterogen memainkan peranan penting dalam membentuk struktur komuniti dan dinamik ekologi yang kompleks.

Kata kunci: persaingan asimetri; pemodelan ekologi; persekitaran heterogen; dinamik batu-kertas-gunting (RPS)

1. Introduction

Cyclic dominance is a core concept in ecological theory, reflecting non-hierarchical interactions where no single species maintains consistent dominance over others. The rock-paper-scissors (RPS) model illustrates this dynamic through a closed-loop system of three species, where each species defeats one competitor while being defeated by another (May & Leonard 1975; Hofbauer & Sigmund 1998; Da Silva *et al.* 2024; Bazeia *et al.* 2025; Justino *et al.* 2025). Despite its simplicity, this model captures essential dynamics observed in diverse ecological and evolutionary systems, such as lizard mating behaviors (Sinervo & Lively 1996), microbial populations and plant competition (Lankau & Strauss 2007).

Environmental heterogeneity adds another layer of complexity to species interactions. Ecological communities are rarely homogeneous, and abiotic gradients such as temperature, nutrient availability, or habitat complexity can alter competitive balances (Chesson 2000; Levine *et al.* 2017). When such environmental variability interacts with asymmetric competition, it can give rise to diverse dynamical outcomes, including spatial separation of species, temporal population cycles, or the emergence of multiple stable states (Durrett & Levin 1998; Kneitel & Chase 2004).

In the pioneering work of May and Leonard (1975), it has been demonstrated that in the case of three competing species, the traditional model of Lotka-Volterra system allows for a unique set of periodic limit cycle solutions. Additionally, they support a broader set of solutions characterized by non-periodic species oscillations with limited amplitude but increasingly longer cycle durations over time. From a biological perspective, this highlights how nonlinear dynamics can create complex behaviors even in basic population models. Mathematically, the system showcases intriguing dynamical behaviors and analytical techniques specific to three-dimensional nonlinear systems. Previous studies of Godsoe *et al.* (2015), employs a simplified Lotka-Volterra competition model, extended across a one-dimensional environmental gradient by letting two-species the carrying capacities to change with locations or abiotic environment. It is shown that how biotic interactions can affect species' range margins and identify situations where small changes in species' interactions dramatically shift these margins.

Asymmetrical rock-paper-scissors (RPS) interactions have been recognized as a key ecological mechanism influencing community structure and diversity (Reichenbach *et al.* 2008; Mohd 2016; Menezes *et* al. 2022; Saburov 2023; Menezes *et al.* 2026). This form of

competition referred to as intransitive competition mirrors the dynamical behavior of rock-paper-scissors game, where each species dominates one and is dominated by another (e.g., rock beats scissors, scissors cuts paper whereas paper cover or wraps rock), for details can be found in the work of Sinervo and Lively (1996). This kind of interactions have been documented in real world ecosystems involving three-species systems (Nahum *et al*. 2011). The foundational RPS system competition model developed by May and Leonard (1975) revealed a range of complex dynamical behaviors, including periodic limit cycles and non-periodic species fluctuations. Distinct modeling studies of RPS systems have also shown that such asymmetric ecological interactions can lead to diverse survival outcomes, such as sustained coexistence among species and multistability, where different single-species dominance states can persist (Park 2021).

In distinct ecological studies (May & Leonard 1975; Mohd *et al.* 2017; Mohd & Park 2021), interspecies competition is generally categorized as either symmetrical interaction where species exert equal competitive pressure on one another or asymmetrical interaction where the intensity of competitive influence differs between species. Previous studies have highlighted the important roles that competitive interactions play in multi-species communities, with much of the focus on two-species (Godsoe *et al.* 2017) and three-species systems (Park *et al.* 2018). While the dynamics of three interacting species have been reasonably well explored in the literatures (Park 2021; Mohd & Park 2021), there remains a gap in understanding and examining how asymmetrical competition such as that seen in rock-paper-scissors interactions operates within homogeneous and heterogeneous environments. Addressing this gap is the central aim of the present ecological dynamics research.

Building on insights from previous research, especially the findings of May and Leonard (1975) we revisit the three-species competitive model extended by Mohd and Park (2021) and examine the system of the model by incorporating environmental gradient to assess how the interplay between abiotic factors and RPS competition system shapes community dynamics. In this study, we examine the joint effects of asymmetric RPS competition model and the steepness of environmental gradients on ecological dynamics. Specifically, we examine the classical RPS framework to incorporate unequal competitive interactions and explore how the change in environmental component influences species persistence and community structure. Using a mathematical modeling approach, we identify multiple dynamical outcomes including species coexistence, limit cycles and heteroclinic cycles revealing how ecological complexity emerges from simple interaction rules under asymmetrical and heterogeneous conditions.

2. Development of the Model

First and foremost, we employ a three species deterministic model extended by Mohd and Park (2021) which is the extension of classical model of Lotka-Volterra competitive system combine with the environmental gradient, x. The model is developed by using the first-order ordinary differential equation for the densities $N_i(t)$ of three-species, defined as follows:

$$\frac{dN_i(t)}{dt} = \frac{r_i N_i(t)}{K_i(x)}\left(K_i(x) - \sum_{j=1}^{3} \alpha_{ij} N_j(t)\right), \quad (i = 1,\ 2,\ 3) \tag{1}$$

where, the function $N_i(t)$ denotes the population density of species i participating in asymmetric cyclic competitive interactions (Rock-Paper-Scissors type), where dominance is intransitive and occurs through competitive suppression rather than predator-prey interactions. The coefficients α_{ij} therefore quantify the strength of interspecific competition among species at the same trophic level and r_i represents the intrinsic growth rate of species i. The parameter

α_{ij} is the competitive effect of species j on species i and it is reflecting realistic ecological differences where the intraspecific competition coefficients, is when $\alpha_{ij} = 1$, for all $i = j$.

The above deterministic ordinary differential equation model assumes that competitive interactions are localized. Species compete through either symmetric interaction (e.g., $\alpha_{ij} = \alpha_{ji} = \alpha$, for any $i \neq$j) or asymmetric interactions (i.e., $\alpha_{ij} \neq \alpha_{ji}$, for any $i \neq j$). This study focuses on a particular form of asymmetric competition known as RPS or intransitive interactions. Species competition outcomes are also influenced by abiotic environmental conditions. To account for this, the model includes an abiotic component, denoted by x, within the carrying capacities $K_i(x)$. Abiotic factors may include temperature, humidity, elevation, and other environmental components. For example, x can represent a geographic location with varying climate, which in turn affects species' presence or absence. The effect of biotic interactions on species distribution may be contingent on how each species response to the environmental gradient, x. To demonstrate these effects of biotic interactions in a multi-species community, we consider and employ a linear environmental gradient, x in a three-species model ($m = 3$). This gradient is integrated into the model by representing the carrying capacities with linear functions, defined as follows:

$$K_i(x) = m_i x + b_i. \tag{2}$$

The linear form of $K_i(x)$ is adopted as a first-order approximation of species' responses to an environmental gradient. This formulation of linear carrying capacities are commonly used in theoretical ecology to capture monotonic environmental trends (e.g., resource availability, temperature, or habitat quality) and serve here as a baseline for comparison with more ecologically realistic nonlinear niche functions, such as quadratic and Gaussian carrying capacities. In particular, the formulation aligns with the approach adopted by (Godsoe *et al.* 2015; Mohd & Park 2021), where linear carrying capacities are employed to systematically explore how environmental gradients interact with asymmetric Rock-Paper-Scissors competition. The parameter m_i describes the rate of change in environmental suitability in response to the abiotic factor, x for the species i and b_i denotes the carrying capacity whenever the environmental gradient is at $x = 0$. Eq. (2) defines the carrying capacity along the environmental gradient x, and this formulation is integrated into the three-species competition model (1) to explore various competitive dynamics among species with differing levels of tolerance to limiting abiotic factor.

The system (1), combined with Eq. (2), introduces a large number of parameters. As it has been described by Mohd and Park (2021) in order to enable a consistent comparison with prior work, specifically the seminal study by May and Leonard (1975) on the classical intransitive system, we adopt the same parameterization settings for the r_i and interspecific competition coefficients α_{ij} such that $r_1 = r_2 = r_3 = 1$, $\alpha_{12} = \alpha_{23} = \alpha_{31} = \alpha$, $\alpha_{21} = \alpha_{32} = \alpha_{13} = \beta$, and $\alpha_{11} = \alpha_{22} = \alpha_{33} = 1$.

To evaluate the robustness of the predictions made by the ML-RPS system May and Leonard, 1975, we relax the assumption of uniformly distributed carrying capacities, specifically $K_i = 1$ for all $i = 1, 2, 3$. Instead, we examine a linear environmental gradient as described in Eq. (2), using the parameter sets $(m_1, m_2, m_3) = (1, 0, 0.9)$ and $(b_1, b_2, b_3) = (0, 0.4, 0)$ as in Mohd and Park (2021). The specific choice of $b_2 = 0.4$ reflects a moderate baseline shift in the carrying capacity of the second species, ensuring that it does not dominate or is overly suppressed in the heterogeneous environment. This value was adopted as an assumption in (Mohd *et al.* 2017), where it was introduced to balance ecological realism with mathematical tractability, allowing species 2 to have a distinct advantage under

certain environmental conditions, while still preserving the intransitive competition structure of the system. Our analytical and numerical investigations are conducted using these environmentally varying carrying capacity parameters, which are inspired by previous modelling efforts (Mohd *et al.* 2017; Park 2021; Mohd & Park 2021). In the following section, we explore this competitive interaction system model by determining its steady states and some other attractors for analysing their stability under the specified conditions.

3. Existence of The Equilibrium Points of Incorporated Model

In this section, we explore the diverse dynamical outcomes of the model (1) under the influence of an environmental gradient, x, as described above. Based on the previously stated parameter choices, the model was simplified to the following set of equations:

$$\begin{aligned}\frac{dN_1}{dt} &= \frac{N_1}{x}(x - N_1 - \alpha N_2 - \beta N_3),\\ \frac{dN_2}{dt} &= \frac{N_2}{0.4}(0.4 - \beta N_1 - N_2 - \alpha N_3),\\ \frac{dN_3}{dt} &= \frac{N_3}{0.9x}(0.9x - \alpha N_1 - \beta N_2 - N_3).\end{aligned} \tag{3}$$

These equations represent the population dynamics of the three competing species along the environmental gradient, incorporating asymmetrical interactions and heterogeneous carrying capacities. By directly solving the above system when $\frac{dN_1}{dt} = \frac{dN_2}{dt} = \frac{dN_3}{dt} = 0$, it is found that the model admits three distinct types of fixed points which can be obtained as follows:

Lemma 3.1. *Eq. (3) admits three categories of fixed points: There are three equilibrium points (absorbing fixed points) each corresponding to a state where only one species persists:*

- $(N_1^*,\ 0,\ 0) = (x,\ 0,\ 0),$ (4)
- $(0,\ N_2^*,\ 0) = (0,\ 0.4,\ 0),$ (5)
- $(0,\ 0,\ N_3^*) = (0,\ 0,\ 0.9x),$ (6)

These represent extinction scenarios where only a single species survives.

Proof. From the first of Eq. (3), we have

$$0 = \frac{N_1}{x}(x - N_1 - \alpha N_2 - \beta N_3)$$

For $(N_1^*,\ 0,\ 0)$, the above equation implies,

$$0 = N_1^* - \frac{N_1^{*2}}{x} = N_1^*\left(1 - \frac{N_1^*}{x}\right).$$

Since $N_1^* \neq 0$, we obtain $N_1^* = x$. Therefore, $(N_1^*,\ 0,\ 0) = (x,\ 0,\ 0)$. From the second of Eq. (3), we have

$$0 = \frac{N_2}{0.4}(0.4 - \beta N_1 - N_2 - \alpha N_3).$$

For $(0,\ N_2^*,\ 0)$, the above equation implies,

$$0 = \frac{N_2^*}{0.4}(0.4 - N_2^*) = N_2^*\left(1 - \frac{N_2^*}{0.4}\right).$$

Since $N_2^* \neq 0$, it follows that $N_2^* = 0.4$. That is $(0,\ N_2^*,\ 0) = (0,\ 0.4,\ 0)$. From the third of Eq. (3), we have

$$0 = \frac{N_3}{0.9x}(0.9x - \alpha N_1 - \beta N_2 - N_3).$$

For $(0,\ 0,\ N_3^*)$, the above equation implies,

$$0 = \frac{N_3^*}{0.9x}(0.9x - N_3^*) = N_3^*\left(1 - \frac{N_3^*}{0.9x}\right).$$

Since $N_3^* \neq 0$, it follows that $N_3^* = 0.9x$. That is $(0,\ 0,\ N_3^*) = (0,\ 0,\ 0.9x)$. □

Lemma 3.2. *Eq. (3) admits three fixed points correspond to the coexistence of any two of the three interacting species. These take the following forms:*

- $(N_1^{**},\ N_2^{**},\ 0) = \left(\frac{2\alpha-5x}{5(\alpha\beta-1)},\ \frac{5\beta x-2}{5(\alpha\beta-1)},\ 0\right)$, (7)
- $(0,\ N_2^{**},\ N_3^{**}) = \left(0,\ \frac{9\alpha x-4}{10(\alpha\beta-1)},\ \frac{4\beta-9x}{10(\alpha\beta-1)}\right)$, (8)
- $(N_1^{**},\ 0,\ N_3^{**}) = \left(\frac{9\beta x-10x}{10(\alpha\beta-1)},\ 0,\ \frac{10\alpha x-9x}{10(\alpha\beta-1)}\right)$, (9)

These equilibria indicate partial coexistence, where only two species persist while the third is excluded.

Proof. From the first of Eq. (3), we have

$$0 = \frac{N_1}{x}(x - N_1 - \alpha N_2 - \beta N_3).$$

For $(N_1^{**},\ N_2^{**},\ 0)$, the above equation implies

$$0 = N_1^{**} - \frac{N_1^{**}}{x} - \frac{\alpha N_1^{**} N_2^{**}}{x} = x - N_1^{**} - \alpha N_2^{**}$$

that is

$$N_1^{**} + \alpha N_2^{**} = x. \tag{10}$$

From the second of Eq. (3), we have

$$0 = \frac{N_2}{0.4}(0.4 - \beta N_1 - N_2 - \alpha N_3).$$

For $(N_1^{**},\ N_2^{**}, 0)$, the above equation implies,

$$0 = N_2^{**} - \frac{\beta\, N_1^{**}\, N_2^{**}}{0.4} - \frac{N_2^{**2}}{0.4} = 0.4 - \beta\, N_1^{**} - N_2^{**}$$

that is

$$\beta\, N_1^{**} + N_2^{**} = 0.4 \tag{11}$$

From the third of Eq. (3), we have

$$0 = \frac{N_3}{0.9x}(0.9x - \alpha N_1 - \beta N_2 - N_3).$$

For $(N_1^{**},\ N_2^{**}, 0)$, the above equation implies,

$$0 = 0$$

Now, combine Eq. (10) and Eq. (11), we have

$$N_1^{**} + \alpha N_2^{**} = x$$
$$\beta\, N_1^{**} + N_2^{**} = 0.4$$

When solving the above equations, it gives

$$N_1^{**} = \frac{2\alpha - 5x}{5(\alpha\beta - 1)}$$

and

$$N_2^{**} = \frac{5\beta x - 2}{5(\alpha\beta - 1)}$$

That is

$$(N_1^{**},\ N_2^{**},\ 0) = \left(\frac{2\alpha - 5x}{5(\alpha\beta - 1)},\ \ \frac{5\beta x - 2}{5(\alpha\beta - 1)},\ 0\right).$$

From the first of Eq. (3), we have

$$0 = \frac{N_1}{x}(x - N_1 - \alpha N_2 - \beta N_3)$$

For $(0,\ N_2^{**},\ \ N_3^{**})$, the above equation implies

$$0 = 0$$

From the second of Eq. (3), we have

$$0 = \frac{N_2}{0.4}(0.4 - \beta N_1 - N_2 - \alpha N_3)$$

For $(0,\ N_2^{**},\ \ N_3^{**})$, the above equation implies,

$$0 = \ N_2^{**} - \frac{N_2^{**2}}{0.4} - \frac{\alpha\ N_2^{**}\ N_3^{**}}{0.4} = 0.4 - \ N_2^{**} - \ \alpha N_3^{**}$$

that is

$$N_2^{**} + \ \alpha N_3^{**} = 0.4 \tag{12}$$

From the third of Eq. (3), we have

$$0 = \frac{N_3}{0.9x}(0.9x - \alpha N_1 - \beta N_2 - N_3)$$

For $(0,\ \ N_2^{**},\ N_3^{**})$, the above equation implies,

$$0 = \ N_3^{**} - \frac{\beta\ N_2^{**}\ N_3^{**}}{0.9x} - \frac{N_3^{**2}}{0.9x} = 0.9x - \beta\ N_2^{**} - \ N_3^{**}$$

that is

$$\beta N_2^{**} + \ N_3^{**} = 0.9x \tag{13}$$

Now, combine Eq. (12) and Eq. (13), we have

$N_2^{**} + \ \alpha N_3^{**} = 0.4$
$\beta N_2^{**} + \ N_3^{**} = 0.9x$

When solving the above equations, it gives

$$N_2^{**} = \frac{9\alpha x - 4}{10(\alpha\beta - 1)} \quad \text{and} \quad N_3^{**} = \frac{4\beta - 9x}{10(\alpha\beta - 1)}$$

That is

$$(0,\ N_2^{**},\ N_3^{**}) = \left(0,\ \frac{9\alpha x - 4}{10(\alpha\beta - 1)}, \frac{4\beta - 9x}{10(\alpha\beta - 1)}\right).$$

From the first of Eq. (3), we have

$$0 = \frac{N_1}{x}(x - N_1 - \alpha N_2 - \beta N_3)$$

For $(N_1^{**},\ 0,\ N_3^{**})$, the above equation implies

$$0 = N_1^{**} - \frac{N_1^{**2}}{x} - \frac{\beta N_1^{**} N_3^{**}}{x} = x - N_1^{**} - \beta N_3^{**}$$

that is

$$N_1^{**} + \beta N_3^{**} = x \tag{14}$$

From the second of Eq. (3), we have

$$0 = \frac{N_2}{0.4}(0.4 - \beta N_1 - N_2 - \alpha N_3)$$

For $(N_1^{**},\ 0,\ N_3^{**})$, the above equation implies,

$$0 = 0$$

From the third of Eq. (3), we have

$$0 = \frac{N_3}{0.9x}(0.9x - \alpha N_1 - \beta N_2 - N_3)$$

For $(N_1^{**},\ 0,\ N_3^{**})$, the above equation implies,

$$0 = N_3^{**} - \frac{\alpha\, N_1^{**}\, N_3^{**}}{0.9x} - \frac{N_3^{**2}}{0.9x} = 0.9x - \alpha\, N_1^{**} - N_3^{**}$$

that is

$$\alpha N_1^{**} + N_3^{**} = 0.9x \tag{15}$$

Now, combine Eq. (14) and Eq. (15), we have

$N_1^{**} + \beta N_3^{**} = x$
$\alpha N_1^{**} + N_3^{**} = 0.9x$

When solving the above equations, it gives

$$N_1^{**} = \frac{9\beta x - 10x}{10(\alpha\beta - 1)} \quad \text{and} \quad N_3^{**} = \frac{10\alpha x - 9x}{10(\alpha\beta - 1)}$$

That is

$$(N_1^{**},\ 0,\ N_3^{**}) = \left(\frac{9\beta x - 10x}{10(\alpha\beta - 1)}, 0, \frac{10\alpha x - 9x}{10(\alpha\beta - 1)}\right). \square$$

Lemma 3.3. *Eq. (3) admits one interior fixed point that corresponds to the coexistence of all three species. This point is of the form:*

$$\frac{(N_1^{***}, N_2^{***}, \ N_3^{***})}{10(\alpha^3-3\alpha\beta+\beta^3+1)}, \tag{16}$$

where the components $N_i^{***}(i = 1,\ 2,\ 3)$ *are given by*

$$N_1^{***} = 9x\alpha^2 - 10x\alpha\beta - 4\alpha + 4\beta^2 - 9x\beta + 10x,$$
$$N_2^{***} = 10x\alpha^2 - 4\alpha\beta - 9x\alpha + 9x\beta^2 - 10x\beta + 4,$$
$$N_3^{***} = 4\alpha^2 - 9x\alpha\beta - 10x\alpha + 10x\beta^2 - 4\beta + 9x.$$

This equilibrium represents complete coexistence, where all three competing species persist in the system under the influence of the environmental gradient and asymmetric interaction coefficients.

Proof. From Eq. (3), we get

$$0 = \frac{N_1}{x}(x - N_1 - \alpha N_2 - \beta N_3),$$
$$0 = \frac{N_2}{0.4}(0.4 - \beta N_1 - N_2 - \alpha N_3),$$
$$0 = \frac{N_3}{0.9x}(0.9x - \alpha N_1 - \beta N_2 - N_3).$$

This implies

$$0 = (x - N_1^{***} - \alpha N_2^{***} - \beta N_3^{***})$$
$$0 = (0.4 - \beta N_1^{***} - N_2^{***} - \alpha N_3^{***})$$
$$0 = (0.9x - \alpha N_1^{***} - \beta N_2^{***} - N_3^{***})$$

By rearranging, we have

$$N_1^{***} + \alpha N_2^{***} + \beta N_3^{***} = x \tag{17}$$
$$\beta N_1^{***} + N_2^{***} + \alpha N_3^{***} = 0.4 \tag{18}$$
$$\alpha N_1^{***} + \beta N_2^{***} + N_3^{***} = 0.9x \tag{19}$$

Solving Eq. (17) and (18) gives

$$(\alpha\beta - 1)N_2^{***} + (\beta^2 - \alpha)N_3^{***} = \beta x - 0.4 \tag{20}$$

Solving Eq. (18) and (19) gives

$$(\alpha - \beta^2)N_2^{***} + (\alpha^2 - \beta)N_3^{***} = 0.4\alpha - 0.9\beta x \tag{21}$$

Combine Eq. (20) and Eq. (21), we have

$$(\alpha\beta - 1)N_2^{***} + (\beta^2 - \alpha)N_3^{***} = \beta x - 0.4$$

$$(\alpha-\beta^2)N_2^{***}+(\alpha^2-\beta)N_3^{***}=0.4\alpha-0.9\beta x$$

Solving the above system, we obtain

$$N_2^{***}=\frac{10\alpha^2x-4\alpha\beta-9\alpha x+9\beta^2x-10\beta x+4}{10(\alpha^3-3\alpha\beta+\beta^3+1)}$$

and

$$N_3^{***}=\frac{4\alpha^2-9\alpha\beta x-10\alpha x+10\beta^2x-4\beta+9x}{10(\alpha^3-3\alpha\beta+\beta^3+1)}$$

Using N_2^{***} and N_3^{***} in Eq. (19), we get

$$N_1^{***}=\frac{9x\alpha^2-10x\alpha\beta-4\alpha+4\beta^2-9x\beta+10x}{10(\alpha^3-3\alpha\beta+\beta^3+1)}.$$

Hence the proof. □

4. Stability Analysis of The Equilibrium Points

Now, the stability of the equilibrium points is examined through the application of linear stability analysis, which uses the Jacobian matrix with entries defined by:

$$\frac{\partial f_i}{\partial N_j}\quad (i,j=1,\ 2,\ 3),$$

where the functions f_i represent the system of differential equations and are defined as follows:

$$f_1=N_1-\frac{1}{x}N_1^2-\frac{\alpha}{x}N_1N_2-\frac{\beta}{x}N_1N_3 \tag{22}$$

$$f_2=N_2-\frac{\beta}{0.4}N_1N_2-\frac{1}{0.4}N_2^2-\frac{\alpha}{0.4}N_2N_3 \tag{23}$$

$$f_3=N_3-\frac{\alpha}{0.9x}N_1N_3-\frac{\beta}{0.9x}N_2N_3-\frac{1}{0.9x}N_3^2 \tag{24}$$

These expressions define the dynamical system, and by evaluating the partial derivatives $\frac{\partial f_i}{\partial N_j}$ at a given fixed point, the Jacobian matrix can be constructed and the eigenvalues of this matrix when obtained would determine the local stability of that equilibrium points.
Accordingly, the Jacobian matrix $J(N_1,\ N_2,\ N_3)$ takes the following form:

$$J(N_1,\ N_2,\ N_3)=\begin{bmatrix}1-\frac{2}{x}N_1-\frac{\alpha}{x}N_2-\frac{\beta}{x}N_3 & -\frac{\alpha}{x}N_1 & -\frac{\beta}{x}N_1\\ -\frac{\beta}{0.4}N_2 & 1-\frac{\beta}{0.4}N_1-\frac{2}{0.4}N_2-\frac{\alpha}{0.4}N_3 & -\frac{\alpha}{0.4}N_2\\ -\frac{\alpha}{0.9x}N_3 & -\frac{\beta}{0.9x}N_3 & 1-\frac{\alpha}{0.9x}N_1-\frac{\beta}{0.9x}N_2-\frac{2}{0.9x}N_3\end{bmatrix}$$

Using the Jacobian framework outlined above, the eigenvalues of the three absorbing fixed points (4), (5) and (6) are obtained as follows:

- For the equilibrium point (4):

$$\lambda_1 = -1, \quad \lambda_2 = 1 - \frac{\beta x}{0.4}, \ \lambda_3 = 1 - \frac{\alpha}{0.9} \tag{25}$$

- For the equilibrium point (5):

$$\lambda_1 = -1, \quad \lambda_2 = 1 - \frac{0.4\alpha}{x}, \ \lambda_3 = 1 - \frac{4\beta}{9x} \tag{26}$$

- For the equilibrium point (6):

$$\lambda_1 = -1, \quad \lambda_2 = 1 - 0.9\beta, \ \lambda_3 = 1 - \frac{9\alpha x}{4}. \tag{27}$$

These eigenvalues would help to analyse the stability of each fixed point based on the signs of λ_2 and λ_3. Similarly, the eigenvalues of the three fixed points correspond to the coexistence of any two of the three interacting species (7), (8) and (9) are as follows:

- For the equilibrium point (7):

$$\lambda_1 = -1, \ \lambda_2 = \frac{4\alpha - 10x + 25\beta x^2 - 10\alpha\beta x}{10x(1-\alpha\beta)}, \ \lambda_3 = \frac{4\alpha^2 - 9x\alpha\beta - 10x\alpha + 10x\beta^2 - 4\beta + 9x}{9x(1-\alpha\beta)} \tag{28}$$

- For the equilibrium point (8):

$$\lambda_1 = -1, \ \lambda_2 = \frac{16\beta - 36x + 81\alpha x^2 - 36\alpha\beta x}{36x(1-\alpha\beta)}, \ \lambda_3 = \frac{9x\alpha^2 - 10x\alpha\beta - 4\alpha + 4\beta^2 - 9x\beta + 10x}{10x(1-\alpha\beta)} \tag{29}$$

- For the equilibrium point (9):

$$\lambda_1 = -1, \ \lambda_2 = \frac{10x\alpha^2 - 4\alpha\beta - 9x\alpha + 9x\beta^2 - 10x\beta + 4}{4(1-\alpha\beta)}, \quad \lambda_3 = \frac{100\alpha + 81\beta - 90\alpha\beta - 90}{90(1-\alpha\beta)}. \tag{30}$$

Similarly, the above eigenvalues help to analyze the stability of each fixed point based on the signs of λ_2 and λ_3.

Finally, the eigenvalues of the interior fixed point that corresponds to the coexistence of all three species (16) are as follows:

$$\lambda_1 = -1$$

$$\lambda_{2,3} = \frac{1}{360x(\alpha^3 - 3\alpha\beta + \beta^3 + 1)} \times (72\alpha + 80\beta - 360x + 200\alpha x + 62\beta x + 405x^2\alpha - 162x\alpha^2 + 180x\alpha^3 + 450x^2\beta - 200x\beta^2 + 180x\beta^3 - 80\alpha^2 - 72\beta^2 - 450x^2\alpha^2 - 405x^2\beta^2) \pm \frac{\frac{1}{2}\left(\sqrt{\frac{\delta_1^2}{32{,}400} + \delta_2\delta_3}\right)}{180x^2(\alpha+\beta-\beta^2+\alpha\beta-\alpha^2-1)^2(\alpha+\beta+1)^2}. \tag{31}$$

These expressions are valid provided the denominator $\alpha^3 - 3\alpha\beta + \beta^3 + 1$ is nonzero to avoid undefined values in the real parts of λ_2 and λ_3. Similar analysis can be found in Mohd and Park (2021).

Theorem 4.1. *Each of the three absorbing fixed points (4), (5), and (6), corresponding to states in which only a single species persists, can be stable provided that all eigenvalues evaluated at the respective fixed points are negative.*

Proof. As shown in Eq. (25), Eq. (26) and Eq. (27) above, the eigenvalue λ_1 is consistently negative for all three fixed points. Therefore, the stability analysis focuses on the signs of λ_2 and λ_3. For fixed point (4), it is evident that both λ_2 and λ_3 can be negative when the conditions $0.4 < \beta x$ and $0.9 < \alpha$ are satisfied, indicating that this fixed point can be stable. Similarly, for the fixed points (5) and (6), if and only if $0.4\alpha > x$, $\frac{9x}{4} < \beta$ and $\frac{10}{9} < \beta$, $\frac{4}{9x} < \alpha$ respectively are satisfied. □

Theorem 4.2. *The two-species coexistence states, in which two out of the three interacting species persist, can be stable provided that all eigenvalues evaluated at the corresponding fixed points are negative.*

Proof. Although the stability conditions for all three two-species fixed points follow a similar approach, we focus here on analysing the stability of fixed points (7), (8) and 9). Here, the stability of these fixed points depends on the value of the parameters (α, β, x). Since the first eigenvalue (λ_1) of each fixed point is negative (-1), then we need to check only for λ_2 and λ_3 in each case. However, this could be done if the numerator and denominator of λ_2 and λ_3 has opposite sign for all the three fixed points, then the two-species steady states can be stable. □

Theorem 4.3. *The interior fixed-point Eq. (16), representing coexistence of all three species, is locally asymptotically stable under suitable parameter conditions.*

Proof. The local stability of the interior fixed point is determined by analysing the eigenvalues of the Jacobian matrix evaluated at that point. The eigenvalues are shown above as Eq. (31), where $\delta_i (i = 1, 2, 3)$ is a polynomial function of x, α and β detailed are in the Appendix. To ensure the eigenvalues $\lambda_{2,3}$ are well-defined, the denominator $\alpha^3 - 3\alpha\beta + \beta^3 + 1$ must be non-zero. It is straightforward to verify that this term vanishes when $\alpha = \beta = 1$. Therefore, to avoid a singularity in the eigenvalue expressions, we restrict our analysis to the domain $(\alpha, \beta) \in \{(x_1, x_2): x_1, x_2 \in R, \text{ and } x_1, x_2 \neq 1\}$. To explore the stability condition, we conduct a numerical analysis by fixing $x = 0.5$ and evaluating the signs of $\lambda_{2,3}$ over a range of values for (α, β). The resulting stability region is illustrated in Figure 1. This numerical evidence confirms that for certain combinations of α and β, all eigenvalues possess negative real parts, indicating that the interior fixed point is locally asymptotically stable. Consequently, the system permits stable coexistence of all three species when environmental and competitive asymmetries are appropriately balanced. □

5. Numerical Results

In this section, we conduct an in-depth numerical investigation to explore the ecological outcomes emerging from asymmetrical rock-paper-scissors (RPS) interactions competition across environmentally heterogeneous landscapes. Our results reveal that the interplay between asymmetrical species interaction and environmental component can drive the emergence of markedly distinct community compositions. Specifically, we observe that asymmetrical RPS dynamics promote the formation of structured coexistence patterns. Furthermore, our simulations uncover a range of coexistence phenomena, wherein gradual changes in environmental or interaction parameters induce qualitative shifts in system behavior such as transitions between stable coexistence equilibria, multistability and other complex attractors.

5.1. *Asymmetric RPS competition with varying α and β in homogeneous environments*

While the simple RPS model of May and Leonard (1975), captures intriguing dynamical features such as oscillatory behavior, its simplifying assumptions particularly the use of identical and constant carrying capacities for all species (e.g., $K_i = 1$, for all $i = 1, 2, 3$) may lead to either an underestimation or overestimation of competitive dynamics. In contrast, adopting a more general asymmetric competition framework is likely to yield qualitatively richer and more ecologically realistic outcomes. This is especially pertinent given that, in natural ecosystems, competitive strengths are rarely asymmetric (Mohd & Park 2021), and added that, species-specific carrying capacities often vary across environmental gradients. Incorporating such ecological asymmetries and heterogeneities into the model enhances its ability to reflect realistic community-level interactions and dynamics (Mohd & Park 2021).

To demonstrate the impact of variable environmental carrying capacities within the three-species system (3), we examine the species interaction dynamics presented in Figure 1 at the position $x = 0.5$, as an example (i.e., the carrying capacities are set to $K_1 = 0.5, K_2 = 0.4$ and $K_3 = 0.45$). This analysis is conducted under the framework of an asymmetric rock-paper-scissors (RPS) competition model, with varying values of the competition parameters α and β. Also, we established the time series and phase space analysis as indicated in Figure 2 to Figure 5 in order to visualize the outcomes illustrated in Figure 1 which are not evident in (Mohd & Park 2021). All the numerical simulations are performed using MATLAB. Phase space trajectories and time-series simulations were additionally verified using the same MATLAB to ensure consistency of the numerical results.

The following Figure 1 maps the long-term dynamical outcomes of the three-species system across a two-parameter space defined by asymmetrical competition strength α and β, both ranging from 0 to 2. The analysis reveals a rich variety of behaviors, from stable coexistence to competitive exclusion and complex oscillations. The top row of Figure 2 indicates the stable coexistence of all three species (cyan), denoted as (N_1, N_2, N_3), is confined to a region of low competition, primarily where $\alpha < 0.8$ and $\beta < 0.7$. The middle row of Figure 2 shows that as competition intensifies, then the stable coexistence of three-species is lost near the central region. Specifically, increasing both parameters leads to a region where species 1 and 3 coexist while species 2 is eliminated (black) i.e., $(N_1, 0, N_3)$. This two-species steady-state is stable within the approximate parameter range of $0.6 < \alpha < 1.0$ and $0.7 < \beta < 1.1$. A smaller adjacent region (pink), supports the coexistence of species 1 and 2, ($N_1, N_2, 0$), and is located approximately between $0.8 < \alpha < 1.1$ and $0.7 < \beta < 0.8$, the time series and the phase space trajectories of this scenario was presented in the last row of Figure 2.

For intense competition scenarios, competitive exclusion becomes the dominant outcome. The victory of species 1 (red) i.e., $(N_1, 0, 0)$, occupies a vast portion of the parameter space, particularly for $\alpha > 1.0$ and $\beta > 0.8$, indicated on the top row of Figure 3. This suggests that

strong symmetrical competition favors species 1. At very high values of both symmetrical and asymmetrical competition, specifically for $\alpha > 1.3$ and $\beta > 1.2$**,** the system enters a bistable state (green) where the initial conditions determine whether species 2 or species 3 ultimately survives (the middle row of Figure 3). A narrow transitional band (gray) separates the regions of species 1 dominance and bistability region and it's visualized in the time series and phase space trajectories on the last row of Figure 3. Furthermore, two extensive regions exhibiting complex oscillatory dynamics are evident. These areas, characterized by finely interwoven color patterns indicative heteroclinic cycles (top and middle rows of Figure 5) and periodic oscillations (last row of Figure 5) are found at high asymmetrical competition. The emergence of these complex dynamics from stable domains highlights that the interplay between symmetrical and asymmetrical competition and environmental carrying capacity is a key mechanism driving the system towards (non-) equilibrium states.

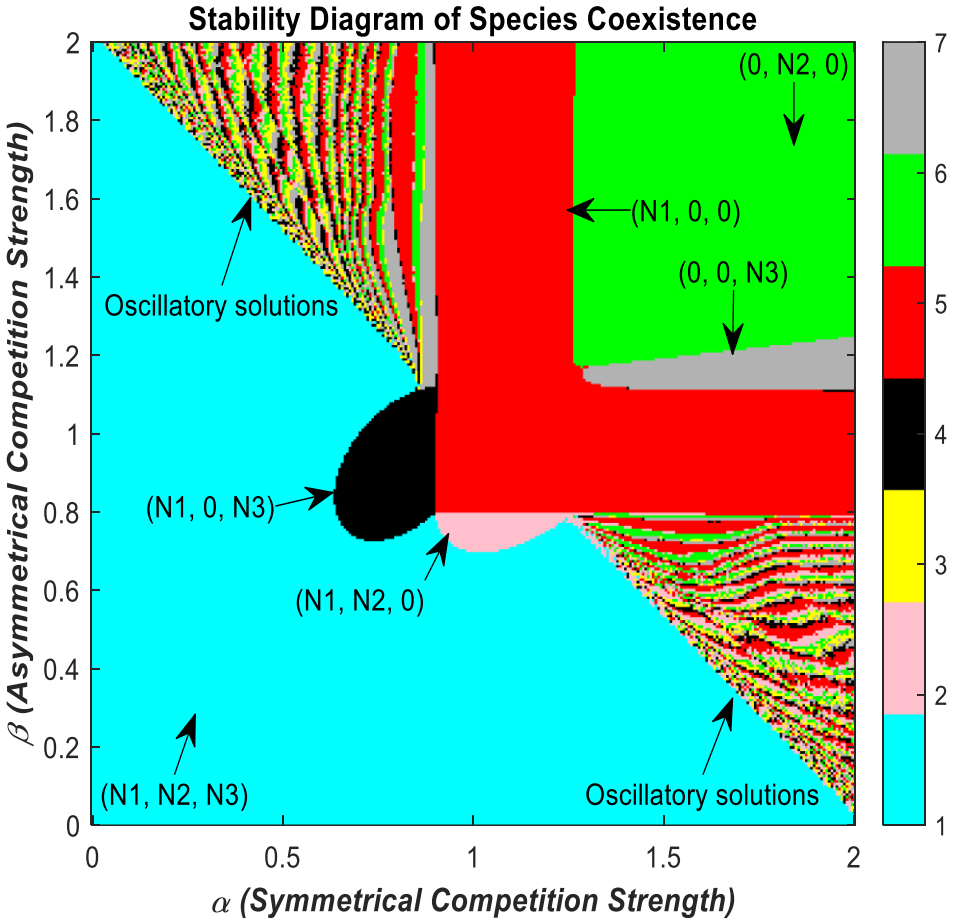

Figure 1: Stability diagram of species coexistence in an asymmetric Rock-Paper-Scissors (RPS) competition model across homogeneous environments. The phase diagram illustrates long-term dynamical outcomes as functions of symmetric competition strength (α) and asymmetric competition strength (β). Different regions are color-coded to represent distinct ecological outcomes: full three species coexistence (cyan), two species coexistence (black, pink), the color map (red, green, gray) represents single species persistence and oscillatory dynamics (striped regions).

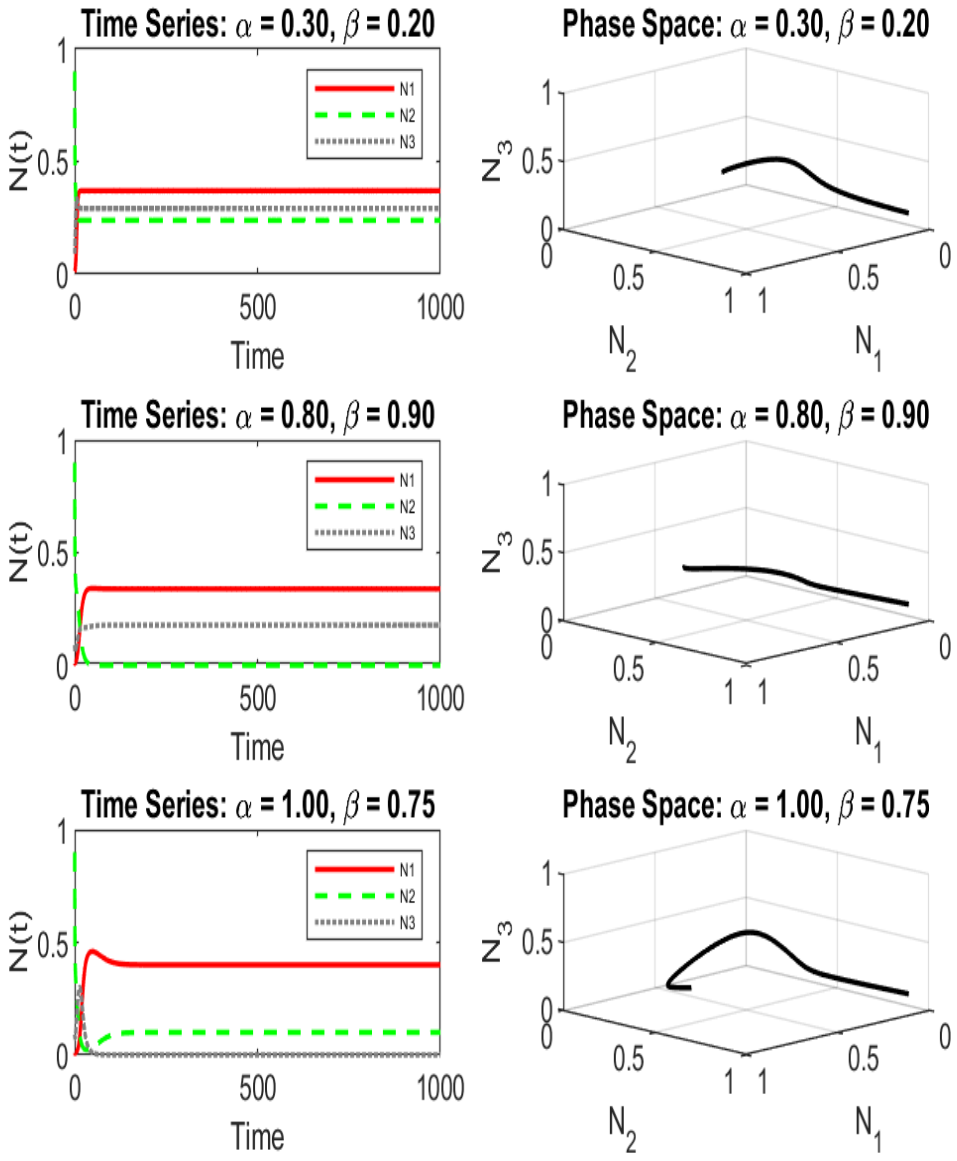

Figure 2: Effect of parameter variations on the three-species system. Each row shows simulations for a parameter pair: time series (left) and phase space trajectories (right). For the first pair, all three species stably coexist, while for the other two pairs the system converges to two-species steady states with one species going extinct, highlighting shifts between different stable attractors.

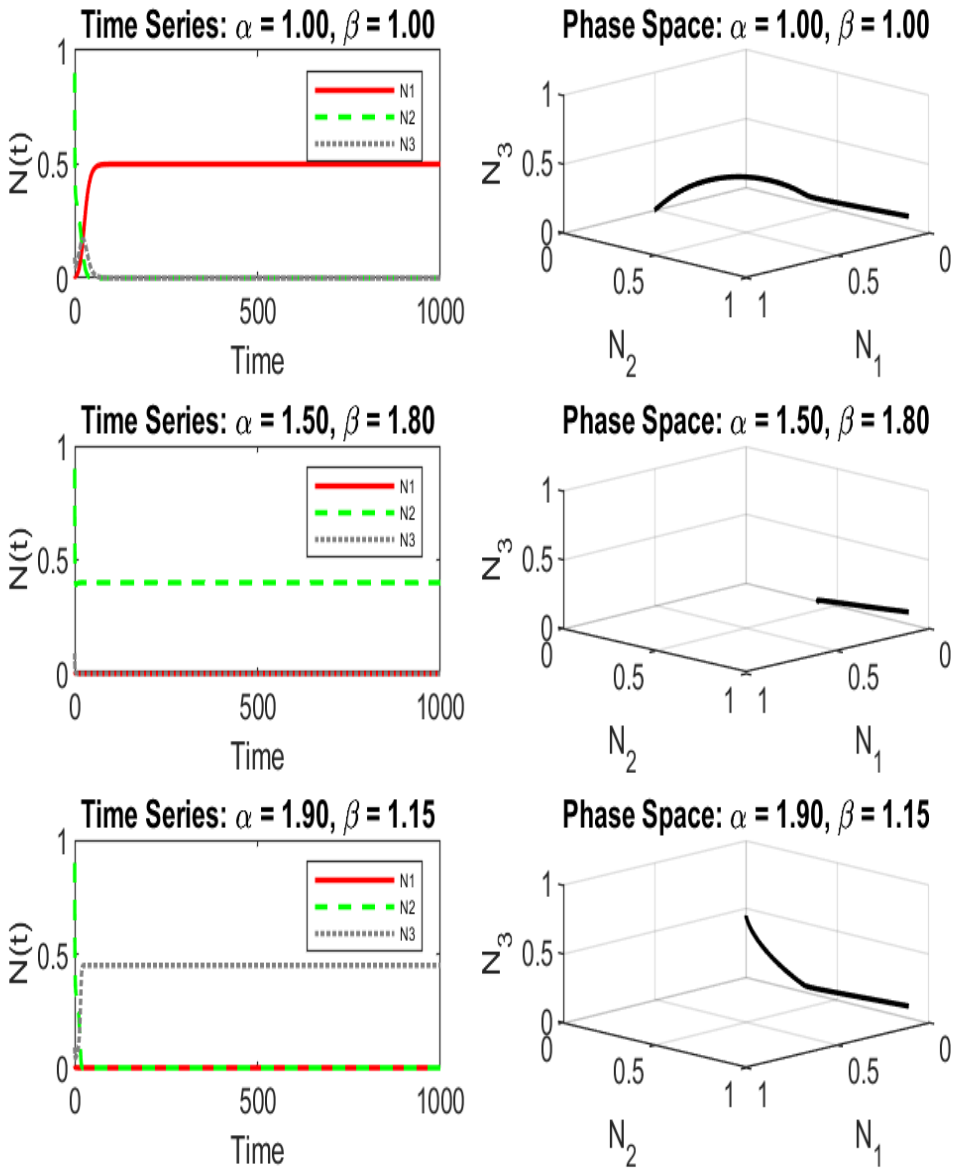

Figure 3: Influence of parameters α and β on the three-species system. Each row shows time series (left: N_1, solid red; N_2, dashed green; N_3, dotted gray) and phase space trajectory (right). For the top row, species N_1 dominates while others go extinct; in the middle row, only N_2 persists (attractor on the N_2-axis); in the bottom row, N_3 outcompetes the others (attractor on the N_3-axis). The system thus converges to stable single-species steady states depending on parameter values.

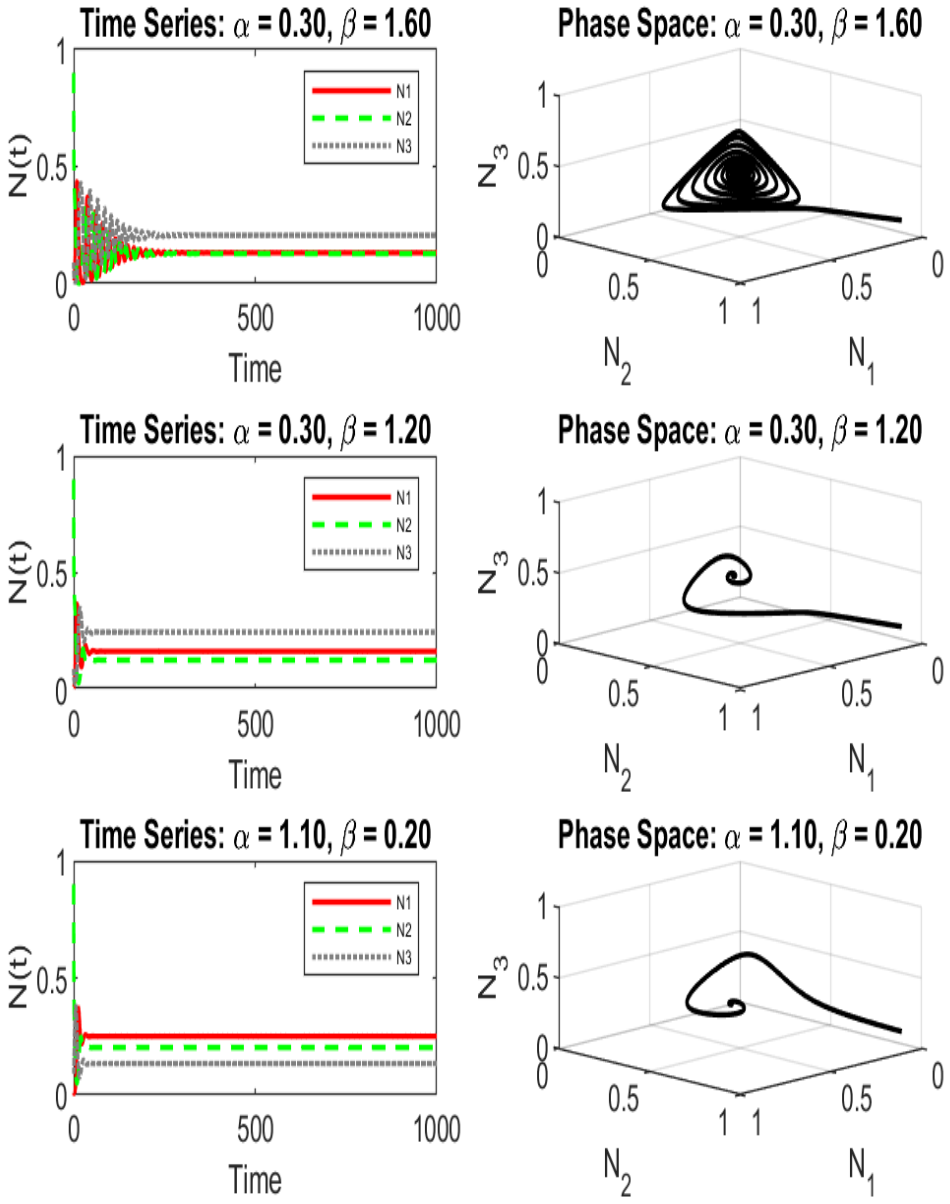

Figure 4: Transition from oscillatory dynamics to stable coexistence under varying parameters α and β with fixed environmental gradient x. For the top row, the system shows sustained oscillations (limit cycle) with dynamic three-species coexistence. For the other parameter sets, oscillations are damped, and trajectories converge to a stable three-species equilibrium. This illustrates a likely supercritical Hopf bifurcation, where decreasing β shifts the system from persistent cycles to a stable steady state (N_1: solid red; N_2: dashed green; N_3: dotted gray).

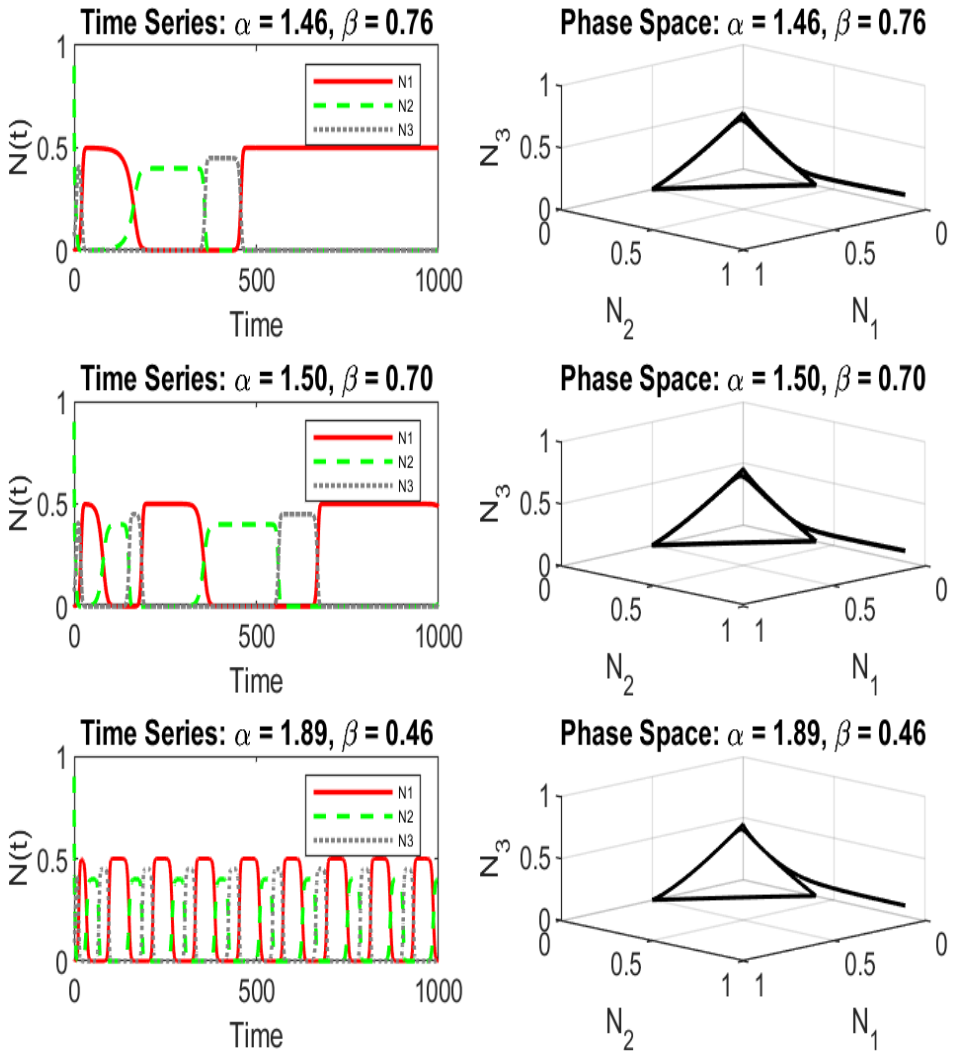

Figure 5: Non-equilibrium dynamics with heteroclinic cycles and limit cycles for three parameter sets. Time series (left) show persistent large-amplitude oscillations with cyclical dominance: species N_1 (solid red), N_2 (dashed green), and N_3 (dotted gray) peak and decline sequentially. Phase space trajectories (right) form triangular loops near the axes, confirming convergence to a stable cycle. While the qualitative outcome is consistent, parameters α and β modulate oscillation features, with shorter periods in the bottom panel. This highlights stable dynamic coexistence rather than static equilibrium.

6. Asymmetric RPS Competition with Varying α and m_3 in Heterogeneous Environments

In this section, we explore the combined influence of asymmetric RPS competition model in heterogeneous environment by varying α and m_3. To achieve this, we perform a two-parameter stability diagram illustrating the system's long-term dynamics by simultaneously varying the asymmetrical competition strength (α) and the environmental sensitivity of species 3 (m_3). This analysis is pivotal for understanding how the interplay between a general competitive structure and individual species' attributes shapes the ecological landscape, determining the conditions

for coexistence, competitive exclusion, and the emergence of complex dynamics. The comprehensive results of this investigation are summarized in the stability diagram presented in Figure 6, which maps the system's long-term asymptotic behavior across the (m_3, α) parameter plane.

6.1. *Numerical results*

Additionally, to assess the effects of spatial variation in environmental carrying capacities within the three-species system (3), we investigate the interaction dynamics displayed in Figure 6 at $x = 0.41$, where in this case, the carrying capacities are specified as $K_1 = 0.41$ and $K_2 = 0.4$. This investigation is framed within an asymmetric rock-paper-scissors (RPS) competition model and explores variations in both the asymmetrical competition strength (α) and the environmental sensitivity of species 3 (m_3). All these outcomes of the following figure is not evident in the simple RPS model with uniform carrying capacities (May and Leonard, 1975), nor in the findings reported by Mohd and Park (2021). Additionally, by varying α and m_3, our analysis reveals the presence of oscillatory dynamics characterized by limit cycles and heteroclinic cycles evident as striped color regions which, to our knowledge, have not been qualitatively identified in any prior studies.

Figure 6 presents the two-parameter stability diagram that portrays the long-term dynamical behavior of the three-species coexistence as a function of the environmental sensitivity of species 3 (m_3) and the strength of asymmetrical competition (α). This analysis reveals a highly structured parameter space where ecological outcomes are intricately determined by the interplay between these two factors. The region shift is characterized by distinct regions of stable coexistence, competitive exclusion, bistability, and complex oscillatory dynamics. The most prominent feature is the large, centrally located domain of stable three-species coexistence (N_1, N_2, N_3), indicated in cyan. This state, representing the highest level of biodiversity, is robust across a wide, continuous range of intermediate environmental sensitivities, approximately $0.25 < m_3 \leq 2$, provided that the asymmetrical competition remains below a critical threshold. The upper boundary of this region follows a distinct convex curve, peaking near $\alpha \approx 1.3$. This shape is highly informative: it demonstrates that as asymmetrical competition (α) increases, the range of environmental sensitivities (m_3) that permits stable coexistence progressively narrows, until the three-species equilibrium is lost entirely through a bifurcation. This illustrates a classic scenario where increasing competitive pressure erodes the parameter space for full coexistence.

Surrounding this core region of stability are several domains of two-species coexistence, highlighting how deviations from the optimal parameter window lead to a sequential loss of species. For low environmental sensitivity $(m_3 < 0.25)$, species 3 is consistently outcompeted, leading to the stable coexistence of species 1 and 2, $(N_1, N_2, 0)$, shown in pink. This outcome persists for asymmetrical competition strengths up to $\alpha \approx 1.0$. Conversely, when the environmental sensitivity of species 3 is high $(m_3 > 1.3)$ and asymmetrical competition is low $(\alpha < 0.7)$, species 1 is driven to extinction, resulting in the stable coexistence of species 2 and 3, $(0, N_2, N_3)$, shown in yellow. A third two-species state, the coexistence of species 1 and 3, $(N_1, 0, N_3)$, appears in a distinct crescent-shaped black region nestled at the upper boundary of the three-species domain for $0.7 < \alpha < 1.4$. The emergence of this state signifies that moderate-to-high asymmetrical competition can selectively destabilize and exclude species 2, even under conditions of intermediate environmental sensitivity for species 3.

In regimes of more extreme parameter values, the system simplifies further into states of single-species dominance or enters complex dynamic states. The large gray region on the right-hand side $(m_3 > 1.4)$ is dominated by outcomes involving species 3, which becomes a superior competitor. Here, we observe both the sole dominance of species 3, $(0, 0, N_3)$, and bistability

with species 2, $(0, N_2, N_3)$, indicating that high environmental sensitivity confers a significant competitive advantage to species 3. In the upper-left quadrant (low m_3, high α), the system favors species 2. The green region shows that as α increases beyond 1.0, the system transitions from a $(0, N_2, N_3)$ state to the complete dominance of species 2, $(0, N_2, 0)$, for $\alpha > 1.7$. Most strikingly, a vast region of non-equilibrium dynamics, (labeled oscillatory solutions), emerges at high asymmetrical competition ($\alpha > 1.3$) for an intermediate range of environmental sensitivities ($0.6 < m_3 < 1.4$). This region's intricate mosaic of colors (red, green, black, etc.) is the hallmark of a complex bifurcational changes in dynamics. This demonstrates that high asymmetrical competition acts as a powerful destabilizing force, fundamentally altering the system's character from stable fixed-point equilibria to a regime of persistent, dynamic fluctuations.

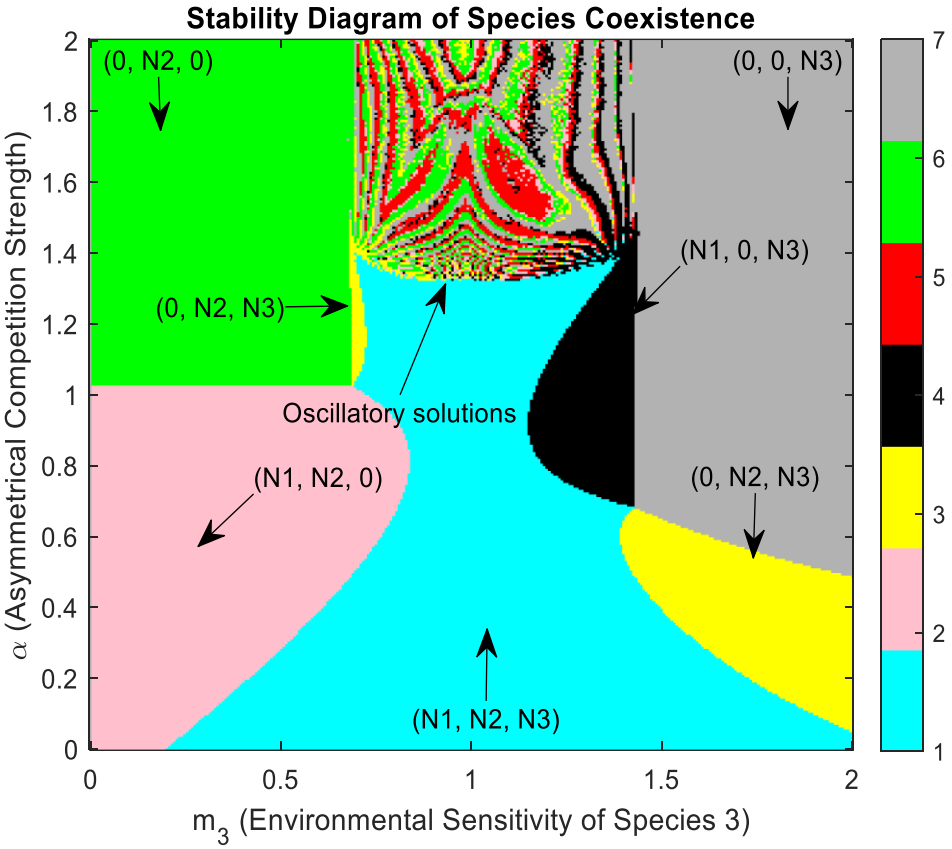

Figure 6: Two-parameter stability diagram of the three-species system as a function of species 3's environmental sensitivity m_3 and asymmetrical competition strength (α). At low values of both parameters, a broad cyan region indicates stable three-species coexistence. Increasing m_3 and α drives bifurcations leading to two-species coexistence (pink, yellow, black) or single-species dominance (green, gray). At high m_3 and intermediate α, a fractal-like region emerges with intermingled basins of attraction, suggesting complex oscillatory or chaotic dynamics. The diagram highlights how rising competitive pressure and environmental sensitivity shift the system from stable equilibria to non-equilibrium behavior.

7. Discussion

Our study of an asymmetrical rock-paper-scissors (RPS) competition model in heterogeneous environments demonstrates that the interplay between unequal competitive strengths and varying environmental conditions generates a wide spectrum of ecological outcomes.

Depending on parameter combinations, the system can stabilize at steady states with single, dual, or full species coexistence, or it can display persistent oscillations. These outcomes are shaped by the interaction between competitive asymmetries and environmental heterogeneity, where small parameter changes can shift community structure across sensitive boundaries, sometimes producing long transients near transition zones.

Ecologically, this highlights distinct mechanisms by which biodiversity can be maintained or lost. The combination of asymmetrical competition and heterogeneous environments shows how communities may move from simple exclusion to complex coexistence. Interpreting the environmental heterogeneity as gradients in species responses emphasizes that even subtle shifts such as those expected under global environmental change can push ecosystems across critical thresholds and into new, potentially less predictable, dynamic regimes.

We also acknowledge limitations in our approach. The model is deterministic and excludes stochastic fluctuations that can be important for small populations or state transitions. Moreover, we focused on a three-species system with simplified functional forms for competition and carrying capacities. Extending these dynamics to more species-rich communities or incorporating stochasticity presents important directions for future work.

Our comprehensive numerical investigation into the three-species ecological model has revealed a remarkably rich and complex landscape of dynamical behaviors, governed by the interplay between symmetrical competition strength (α), asymmetrical competition strength (β), and the environmental sensitivity of species 3 (m_3). The results systematically demonstrate that the long-term ecological outcome ranging from stable coexistence to competitive exclusion and persistent oscillations is not an intrinsic property of the community but is highly contingent upon these key parameters. The system exhibits multiple coexisting attractors, meaning that for a given set of parameters, the final state can depend on the initial population densities, although our analysis focused on the attractors themselves.

The primary finding is the demonstrations of distinct dynamical regimes within the parameter space. We identified broad regions supporting stable, multi-species coexistence, either with all three species persisting at an equilibrium (an interior fixed-point attractor) or with two species coexisting on a boundary plane following the exclusion of the third. These equilibrium states represent classical ecological outcomes. However, a significant portion of the parameter space gives rise to oscillatory dynamics. We consistently observed the emergence of stable limit cycles, where populations engage in sustained, regular oscillations. The aperiodic solutions, particularly the heteroclinic cycles, represent a form of dynamic coexistence where only single-species persist. This finding highlights the critical role that non-equilibrium mechanisms can play in maintaining biodiversity, a concept of central importance in theoretical ecology.

The two-parameter stability diagram provides a powerful synthesis of these findings, mapping the system's asymptotic behavior across the (α, m_3) plane. This map not only confirms the existence of well-defined regions for various exclusion and coexistence scenarios but also highlights the nature of the transitions between them. The sharp, clear boundaries between many regions correspond to critical bifurcation points, where a small change in a parameter can induce a sudden, qualitative shift in the ecosystem's structure for instance, from three-species coexistence to the abrupt loss of a species. Of particular significance is the intricate, interwoven the region at high competition strength, which indicates extreme sensitivity to initial perturbations and suggests the presence of non-equilibrium dynamics like heteroclinic cycles. This outcome represents a regime where long-term prediction becomes practically harder to anticipate, and community structure is inherently unpredictable and complex.

8. Conclusion

In conclusion, this study demonstrates that asymmetrical RPS competition in heterogeneous environments can produce a wide range of ecological scenarios. The system can stabilize in single-, two-, or three-species steady states, exhibit stable limit cycles with periodic fluctuations, or display transient heteroclinic cycles and alternative stable states where the outcomes depend on initial conditions. These results show that even a deterministic three-species model can capture dynamics spanning from simple equilibria to complex, non-equilibrium attractors.

Our findings emphasize three key insights: (i) community structure and stability critically depend on the strength and asymmetry of interspecific interactions under environmental heterogeneity; (ii) coexistence may be dynamically sustained through oscillations rather than only stable equilibria; and (iii) transitions between states can be abrupt or continuous, indicating potential ecosystem vulnerability near bifurcation thresholds.

This work contributes a theoretical framework for understanding biodiversity maintenance and stability in complex ecosystems, while underscoring the risk of sudden community shifts under subtle environmental change. Future research should experimentally validate these dynamic regimes, incorporate stochastic effects, and extend the model to nonlinear gradients and higher-dimensional systems to enhance real-world applicability.

Acknowledgement

The second author is supported by the Universiti Sains Malaysia Research University Team (RUTeam) Grant Scheme (Grant Number: 1001/PMATHS/8580042).

References

Bazeia D., Ferreira M.J.B., de Oliveira B.F. & dos Santos W.A. 2025. Monitoring biodiversity on highly reactive rock-paper-scissors models. *Applied Mathematics and Computation* **502**: 129474.

Chesson P. 2000. Mechanisms of maintenance of species diversity. *Annual Review of Ecology and Systematics* **31**(1): 343–366.

Da Silva R.R.J. 2024. Critical phenomena in rock-paper-scissors model. Master Thesis. Universidade Federal de São Carlos.

Durrett R. & Levin S. 1998. Spatial aspects of interspecific competition. *Theoretical Population Biology* **53**(1): 30–43.

Godsoe W., Murray R. & Plank M.J. 2015. Information on biotic interactions improves transferability of distribution models. *The American Naturalist* **185**(2): 281–290.

Godsoe W., Holland N.J., Cosner C., Kendall B.E., Brett A., Jankowski J. & Holt R.D. 2017. Interspecific interactions and range limits: Contrasts among interaction types. *Theoretical Ecology* **10**(2): 167–179.

Hofbauer J. & Sigmund K. 1998. *Evolutionary Games and Population Dynamics*. Cambridge, UK: Cambridge University Press.

Justino R.R., de Oliveira B.F. & dos Santos F.E.A. 2025. Critical phenomena in the rock-paper-scissors model. *Physica A: Statistical Mechanics and Its Applications* **680**: 131018.

Kneitel J.M. & Chase J.M. 2004. Trade-offs in community ecology: Linking spatial scales and species coexistence. *Ecology Letters* **7**(1): 69–80.

Levine J.M., Bascompte J., Adler P.B. & Allesina S. 2017. Beyond pairwise mechanisms of species coexistence in complex communities. *Nature* **546**(7656): 56–64.

Lankau R.A. & Strauss S.Y. 2007. Mutual feedbacks maintain both genetic and species diversity in a plant community. *Science* **317**(5844): 1561–1563.

Mohd M.H. & Park J. 2021. The interplay of rock-paper-scissors competition and environments mediates species coexistence and intriguing dynamics. *Chaos, Solitons & Fractals* **153**: 111579.

Mohd M.H., Murray R., Plank M. J. & Godsoe W. 2017. Effects of biotic interactions and dispersal on the presence-absence of multiple species. *Chaos, Solitons & Fractals* **99**: 185–194.

Mohd M.H.B. 2016. Modelling the presence-absence of multiple species. PhD Thesis. University of Canterbury.

May R.M. & Leonard W. J. 1975. Nonlinear aspects of competition between three species. *SIAM Journal on Applied Mathematics* **29**(2): 243–253.

Menezes J., Barbalho R. & Sun Y. 2026. Saltatory targeting strategy in rock–paper–scissors models. *Chaos, Solitons & Fractals* **202**: 117450.
Menezes J., Rangel E. & Moura B. 2022. Aggregation as an antipredator strategy in the rock-paper-scissors model. *Ecological Informatics* **69**: 101606.
Nahum J.R., Harding B.N. & Kerr B. 2011. Evolution of restraint in structured rock-paper-scissors community. *Proceedings of the National Academy of Sciences* **108**(supplement_2): 10831–10838.
Park J. 2021. Evolutionary dynamics in the rock-paper-scissors system by changing community paradigm with population flow. *Chaos, Solitons & Fractals* **142**: 110424.
Park J., Do Y. & Jang B. 2018. Multistability in the cyclic competition system. *Chaos: An Interdisciplinary Journal of Nonlinear Science* **28**(11): 113110.
Reichenbach T., Mobilia M. & Frey E. 2008. Self-organization of mobile populations in cyclic competition. *Journal of Theoretical Biology* **254**(2): 368–383.
Saburov M. 2023. Historic behavior in rock–paper–scissor dynamics. *Qualitative Theory of Dynamical Systems* **22**(3): 121.
Sinervo B. & Lively C.M. 1996. The rock-paper-scissors game and the evolution of alternative male strategies. *Nature* **380**(6571): 240–243.

Department of Mathematics and Statistics
Faculty of Natural and Applied Sciences
Umaru Musa Yar'adua University
P.M.B. 2218, Dutsin-ma Road
820102, Katsina, NIGERIA
E-mail: tasiu.abdullahi@umyu.edu.ng

School of Mathematical Sciences
Universiti Sains Malaysia
11800 USM
Penang, MALAYSIA
*E-mail: tasiu@student.usm.my, mohdhafizmohd@usm.my**

Received: 30 June 2025
Accepted: 31 January 2026

*Corresponding author